

## Adsorption isotherms and kinetics of acid violet 48 onto sludge-straw adsorbent

Xiao Li Ren\*, Xue Hui Lai, Yao Sun, Dong Liang He, Juan Lei

Department of Environment and Safety Engineering, Taiyuan Institute of Technology, Taiyuan Shanxi 030008, China, Tel. +86 (0351) 3566125, Fax. +86 (0351) 3566100, email: xren66@126.com (X.L. Ren), 447960078@qq.com (X.H. Lai), 373820760@qq.com (Y. Sun), 418631947@qq.com (D.L. He), 471170382@qq.com (J. Lei)

Received 14 December 2015; Accepted 3 December 2016

### ABSTRACT

The sludge-straw adsorbent was prepared by chemical pyrolysis and characterized by Brunauer Emmett Teller (BET), T-plot, Barrette Joynere Halenda (BJH), scanning electron microscope (SEM) and Fourier transform infrared red (FTIR) spectrometer. Batch experiments were conducted to evaluate the effect of temperature, contact time, initial dye concentration, pH and adsorbent dose. Adsorption mechanism of acid violet 48 onto the sludge-straw adsorbent had been discussed preliminarily on the basis of different kinetics and adsorption isotherm models. The results showed that the pseudo-second order adsorption mechanism was predominant. The maximum adsorption capacity obtained from Langmuir model was 833.33 mg/g at 308 K. Isotherm parameters were calculated, the results indicated that the adsorption processes were endothermic ( $\Delta H > 0$ ), spontaneous ( $\Delta G < 0$ ) and accompanied by an increase in randomness ( $\Delta S > 0$ ).

*Keywords:* Acid violet 48; Adsorption; Isotherm; Thermodynamic; Kinetic

### 1. Introduction

Nowadays, large amounts of wastewater are discharged from the printing and dyeing industry, which contains a lot of water pollutants, such as dyes, pastes, additives, fiber impurities, sand, inorganic salt and so on. Among them, dyes are considered as the most severe contaminant of wastewater. The dyes in wastewater contain toxic organic compounds and substances. Being discharged into water streams, they would be harmful to environment and be a carcinogen and mutagen for humans through contaminated drinking water [1]. Most dyes are usually composed of aromatic nucleus, which are inert and non-biodegradable. A wide range of physicochemical techniques, such as chemical oxidation, flocculation, photo-degradation, adsorption, and membrane separation, coagulation and ion-exchange have been employed to treat print and dye wastewater. Among them, adsorption technique is the most attractive and effective method for removal of organic dyestuffs from the wastewater due to its low initial cost, simple operation, and insensitivity to toxic pollutants, etc [2,3].

As we all know, conventional activated carbon derived from high quality coal or shell is the most widely used adsorbent. Because of its micro-porous structure, high adsorption capacity and extraordinary surface area, activated carbon has a good adsorption effect on the purification of wastewater. However, the higher cost limits its application in wastewater treatment. This has led to the continuous search for easily obtainable and cost-effective adsorption materials. Lots of research has been done to find alternative adsorbents from other materials. A large number of industrial and agricultural waste materials have been successfully utilized as potential adsorbents for the removal of dyes and pigments from wastewater, such as perlite [4], chitosan [5–7], pyrolyzed petrified sediment [8], wheat bran [9], rice husk [10], wood and wood sawdust [11,12], camellia seed powder [13], Platanus orientalis leaf powder [14], clays [15,16], phosphate [17], Eichhornia plant [18–20], kaolinite and montmorillonite [21], fish bone [22], sepiolite [23], hen feather [24–27], peanut husk [28,29], etc.

Excess sludge is the solid waste generated during the process of wastewater treatment. In recent years, the accelerated process of urbanization and industrialization leads to the

\*Corresponding author.

increase of sewage sludge production, and how to deal with the excess sludge caused the attention of the environmental researchers. Because the excess sludge is rich in organic matter, it can be converted into porous absorbing materials, which meets the idea of sustainable development [30,31].

In this paper, the excess sludge was prepared into the adsorbent by dried pyrolysis. The corn straw, a surplus agricultural byproduct was added to improve the adsorption performance in the preparation process of adsorbents, considering that the fixed carbon content of the excess sludge is low. The adsorption isotherms and kinetics of acid violet 48 onto sludge-straw adsorbent were investigated, which was important to identify various natural environmental systems. The thermodynamic activation parameters of the process, such as activation energy, enthalpy, entropy and free energy, were also determined.

## 2. Materials and methods

### 2.1. Materials

Acid violet 48 was purchased from Sinopharm Chemical Reagent Co., Ltd, China. The purity of the material is more than 99%. The molecular formula of acid violet 48 is  $C_{37}H_{38}N_2Na_2O_9S_2$ , the molecular weight is 764.82, and the CAS number is 12220-51-8.

The stock solution of acid violet 48 (1000 mg/L) was prepared by dissolving a required amount of dye powder in deionized water, and the working solutions were freshly prepared by diluting the stock solution with deionized water.

The excess sludge was obtained from the northern suburban wastewater treatment plant of Taiyuan city in Shanxi province, North China. The sludge-straw adsorbents were prepared by dry pyrolysis method. The  $N_2$  adsorption-desorption isotherms of the adsorbent were measured using an automatic adsorption instrument (ASAP 2020 M, Micro-meritics Instrument Co., USA) at liquid nitrogen temperature ( $N_2$ , 77K) [32,33]. The morphologies and structures of the adsorbent and sludge were observed by scanning electron microscope (Hitachi S-4800, Japan).

### 2.2. Batch experiment

Batch equilibrium experiments were investigated using a series of dye-solutions with the initial concentration ranging from 170 to 560 mg/L. The adsorbent dose was 0.5 g/L and agitated for 12 h. After the adsorption for 12 h, the concentrations in the residual dye-solutions were measured using the UV-VIS spectrophotometer UV-2100PC scanning spectrum at the maximum absorbance wavelengths of 530 nm. The amount of the adsorbed dyes ( $q_e$ , mg/g) at equilibrium on the sludge-straw adsorbent was determined by the mass balanced equation Eq. (1):

$$q_e = \frac{(C_0 - C_e) \times V}{M} \quad (1)$$

where  $C_0$  and  $C_e$  are the initial and equilibrium liquid-phase concentrations of dyes (mg/g),  $M$  is the mass of adsorbent (g) and  $V$  is the volume of the solutions (L).

Batch kinetic experiments were conducted in an oscillation incubator at 296 K. The initial dye concentration was

100, 200 and 300 mg/L respectively with the adsorbent dose of 0.8 g/L. The solution samples were separated at predefined time intervals and determined. The adsorption capacity ( $q_t$ , mg/g) at time was calculated by using Eq. (2):

$$q_t = \frac{(C_0 - C_t) \times V}{M} \quad (2)$$

where  $q_t$  is the amount of dye adsorbed at time (mg/g),  $C_t$  is the dye concentration at time (mg/L).

## 3. Results

### 3.1. Characteristics of sludge-straw adsorbent

The  $S_{BET}$  of the adsorbent was  $459.77 \text{ m}^2/\text{g}$ , and micro-pore volume ( $V_{mi}$ ) was  $0.164 \text{ cm}^3/\text{g}$  obtained by the t-pot method.

FT-IR analysis was carried out to evaluate the change of functional groups situated on the surface of adsorbent compared to straw and excess sludge.

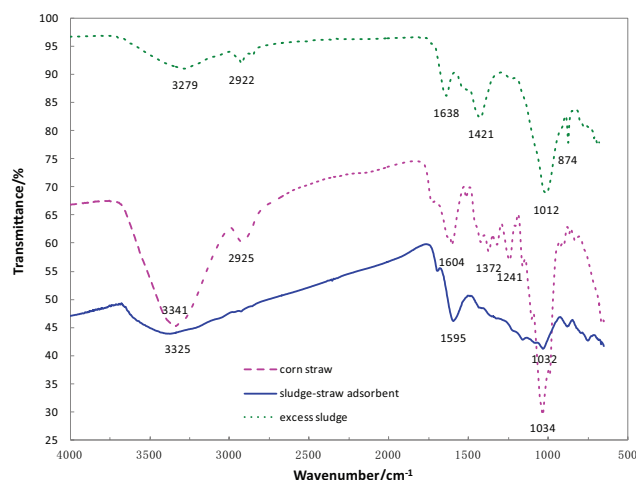


Fig. 1. FT-IR spectra of adsorbent and materials.

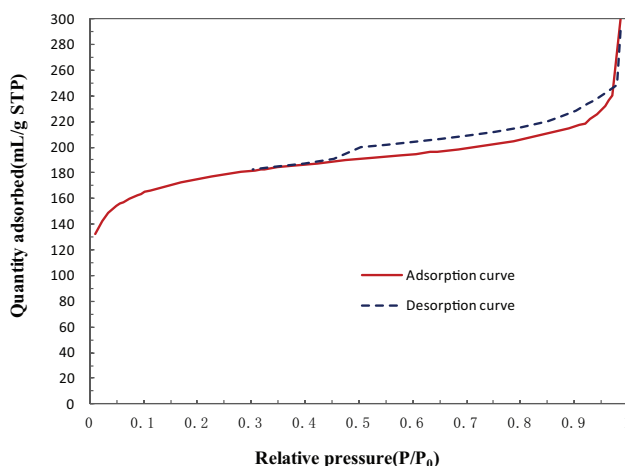


Fig. 2. Adsorption and desorption isotherms of the sludge-straw adsorbent.

It can be seen from the FTIR spectra in Fig. 1, the bands at about  $3279\text{ cm}^{-1}$  (excess sludge),  $3325\text{ cm}^{-1}$  (sludge-straw adsorbent) and  $3341\text{ cm}^{-1}$  (straw) corresponds to the stretching vibrations of surface hydroxyl groups. The bands at about  $2922\text{ cm}^{-1}$  (excess sludge) and  $2925\text{ cm}^{-1}$  (straw) could be assigned to C–H vibration which indicated that excess sludge and corn straw contains organic matter. This band disappeared in the FTIR spectra of sludge-straw adsorbent, which illustrated that the C–H bond had been destroyed in the process of the formation of the adsorbent. The bands at  $1638\text{ cm}^{-1}$  (excess sludge),  $1595\text{ cm}^{-1}$  (sludge-straw adsorbent) and  $1604\text{ cm}^{-1}$  (straw) could be assigned to  $\text{C}=\text{C}$ - or  $\text{C}=\text{O}$  groups. The bands at about  $1012\text{ cm}^{-1}$  (excess sludge),  $1032\text{ cm}^{-1}$  (sludge-straw adsorbent) and  $1034\text{ cm}^{-1}$  (straw) might be attributed to the structure of C–O–C groups. Compared to the excess sludge and the corn straw, the peak intensity at about  $1032\text{ cm}^{-1}$  decreased, which indicated that the C–O–C groups were destroyed in the pyrolysis process.

As seen from Fig. 2, the isotherm of the sludge-straw adsorbent was similar to type I character as defined by International Union of Pure and Applied Chemistry (IUPAC) classification, corresponding to the Langmuir monolayer adsorption process, and the adsorption was reversible and occurred mainly within micro-pores. When  $P/P_0$  was close to 1, the isotherm increased rapidly, owing to the gaps between the particles.

It can be seen from Fig. 3, the sludge-straw adsorbent exhibited a narrow mesopore distribution, with a peak occurring about 1.9 nm.

Fig. 4a and 4b show the scanning electron microscope (SEM) photograph of the surplus sludge and the adsorbent respectively.

The SEM image of the adsorbent shows a very large number of pores, by contrast with the SEM image of the surplus sludge. This demonstrates that the materials can form well-developed pore structures after carbonization and activation.

### 3.2. Effect of temperature and initial concentration

Fig. 5 shows the adsorption capacity of acid violet 48 at different temperatures ( $15^\circ\text{C}$ ,  $25^\circ\text{C}$  and  $35^\circ\text{C}$ ) by plotting its  $q_e$  vs.  $C_0$  at the adsorbent dose of  $0.5\text{ g/L}$ .

When the temperature was raised from 288 to 318 K, the uptake capacity of acid violet 48 increased, indicating that

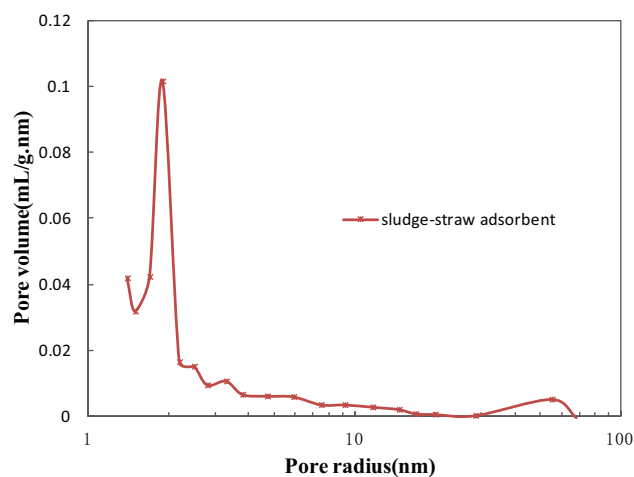


Fig. 3. BJH distribution curve.

the adsorption was an endothermic process in nature. This could be attributed to the increasing of dye diffusion rate across the external boundary layer and in the internal pores of the adsorbent particle at higher temperature. In addition, increasing the initial concentration of dye will make the adsorption capacity of acid violet 48 increase.

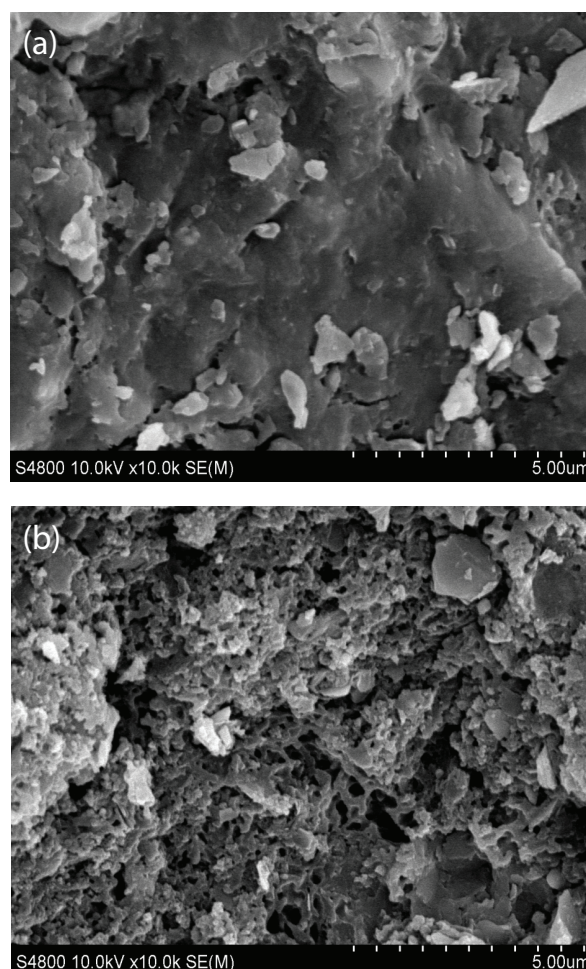


Fig. 4. SEM image of the surplus sludge and the adsorbent.

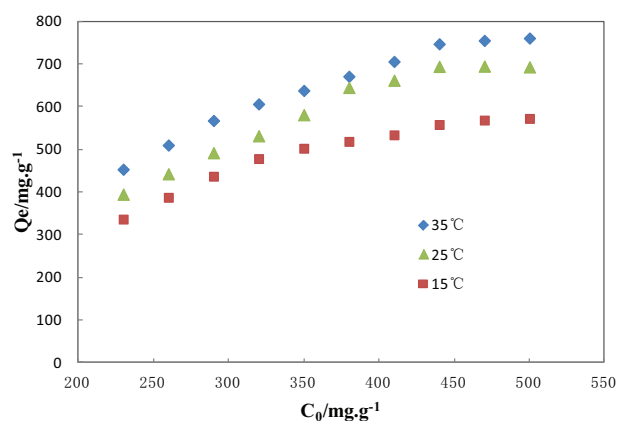


Fig. 5. The effect of temperature on the adsorption capacity.

### 3.3. Effect of contact time and initial concentration

Fig. 6 shows the adsorption amount of acid violet 48 as a function of contact time at 100, 200 and 300 mg/L initial concentration under 296 K, respectively.

It was observed that the adsorption amount of acid violet 48 onto sludge-straw adsorbent increased quickly with increasing contact time at first, and then the adsorption rate increased slowly until the equilibrium was achieved. This may be attributed to large available amounts of adsorption sites on the surface of adsorbent. As the adsorption sites became gradually filled up, the adsorption rate decreased [2]. The equilibrium time was 225, 480 and 660 min for 100, 200 and 300 mg/L initial concentration, respectively.

### 3.4. Effect of solution pH and the dosage

Fig. 7a and 7b show the effect of the solution pH and adsorbent dosage on removal rate of acid violet 48.

It was observed from Fig. 7a that the removal rate of dye was found to decrease with increasing pH and it decreased from 82.65% to 44.05% for an increase in pH from 3 to 10. The figure demonstrated that the removal rate decreased with increasing pH because of the electrostatic attraction between the dye and the positively charged adsorbent surface. As the pH increases from 3 to 10, the number of ionisable sites on adsorbent surface increases. Fig. 7b shows that the removal rate of acid violet 48 increased with increasing dosage of the sludge-straw adsorbent. When the dosage achieved 0.1 g/L, the removal rate approached nearly 100%.

### 3.5. Adsorption isotherms

For the equilibrium isotherm assessment, the Langmuir, Freundlich and Tempkin isotherm models were used to analyze the experimental data.

The linear form of Langmuir isotherm model given below was used by plotting  $C_e/Q_e$  against  $C_e$  [34]:

$$\frac{C_e}{Q_e} = \frac{1}{Q_m K_L} + \frac{C_e}{Q_m} \quad (3)$$

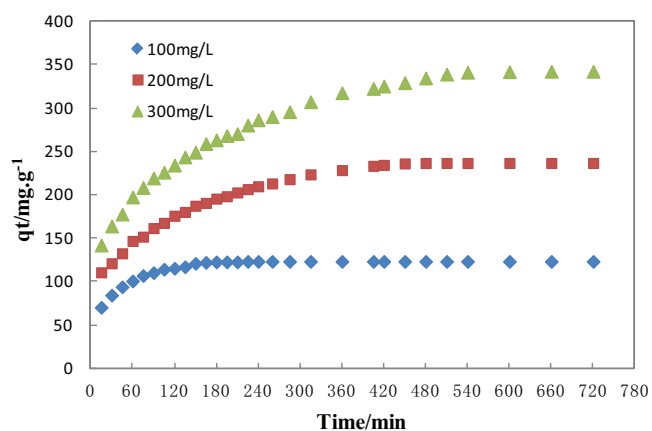


Fig. 6. Adsorption amount of acid violet 48 on sludge-straw adsorbent as a function of contact time (Adsorbent dose = 0.8 g/L,  $T = 296$  K).

where  $C_e$  (mg/L) is the equilibrium concentration of the dye,  $Q_e$  (mg/g) is the adsorption capacity at equilibrium,  $Q_m$  (mg/g) is maximum monolayer adsorption capacity, and  $K_L$  (L/mg) are the Langmuir constants related to maximum monolayer adsorption capacity.  $Q_m$  and  $K_L$  for the model can be obtained from the slope and intercept of the plot.

The linear form of Freundlich isotherm model given below was used by plotting  $\ln Q_e$  against  $\ln C_e$  [35]:

$$\ln Q_e = \ln K_F + \frac{1}{n} \ln C_e \quad (4)$$

where  $K_F$  and  $n$  are Freundlich constants, representing adsorption capacity and adsorption intensity respectively, and can be estimated from the intercept and slope of the linear plots of  $\ln Q_e$  vs.  $\ln C_e$ . For favorable adsorption,  $n$  is  $< 1$ .

The linear form of Tempkin isotherm model given below was used by plotting  $Q_e$  against  $\ln C_e$ :

$$Q_e = \frac{RT}{B} \ln C_e + \frac{RT}{B} \ln A \quad (5)$$

where  $A$  and  $B$  are Tempkin constants.

The Langmuir model is based on the assumption that adsorption is localized on a monolayer and all adsorption sites at the adsorbent are homogeneous [36]. Whereas

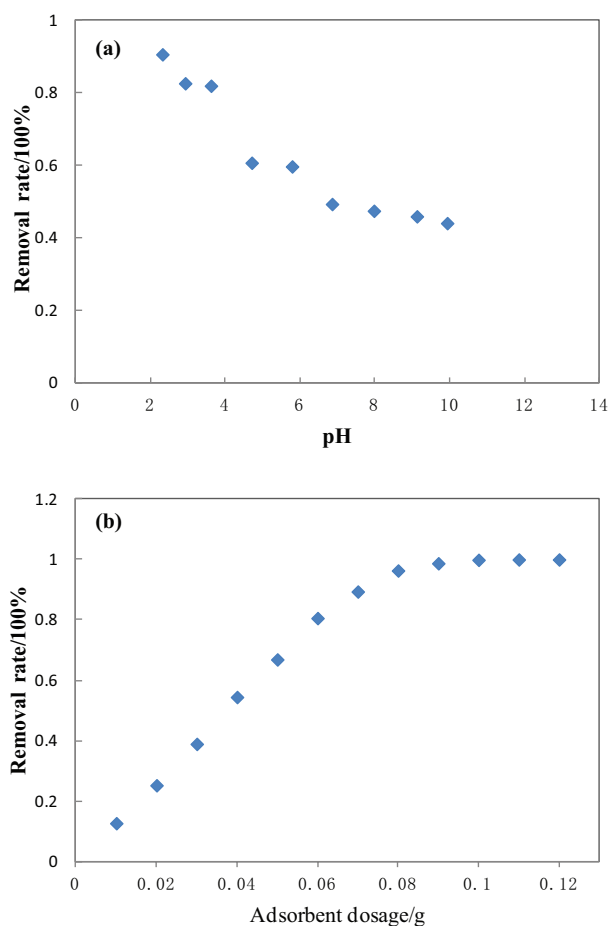


Fig. 7. The effect of pH (a) and adsorbent dosage (b) on removal rate of acid violet 48.

the Freundlich model presumes that the multilayer of the adsorption process occurs on a heterogeneous surface [37]. The Tempkin model considers effects of indirect adsorbate/adsorbent interactions and suggests that because of these interactions the heat of all the molecules in the layer will decrease linearly with coverage. The Langmuir, Freundlich and Tempkin isotherm linear plots for the adsorption of acid violet 48 were shown in Figs. 8–10, and isotherm parameters for the adsorption of acid violet 48 at different temperatures were listed in Table 1.

As shown in Figs. 8–10 and Table 1, the adsorption isotherm of acid violet 48 onto the sludge-straw adsorbents is better fitted to the Langmuir isotherm model ( $R = 0.999, 0.999, 0.999$ ) than the Freundlich isotherm ( $R^2 = 0.951, 0.968, 0.980$ ) and the Tempkin isotherm ( $R^2 = 0.965, 0.965, 0.988$ ). Langmuir equation parameters  $Q_m$  increase in accordance with the increase of temperature, which implies that a higher temperature is more conducive to adsorption. The concentration index of the Freundlich model  $1/n$  is between 0.1 and 0.2, indicating the adsorption was favorable.

### 3.6. Adsorption thermodynamics

The thermodynamic adsorption parameters,  $\Delta H^0$ ,  $\Delta S^0$  and  $\Delta G^0$  (Table 2), were computed from the plots of  $\ln K_d$  vs.  $1/T$  from the equations. The thermodynamic model given below was used by plotting  $\ln K_d$  against  $1/T$ . Thermodynamic parameters were obtained from the slope and intercept of the plot:

$$\ln K_d = \frac{\Delta S^0}{R} - \frac{\Delta H^0}{RT} \quad (6)$$

And the Gibbs free energy was determined from the Eq. (7):

$$\Delta G^0 = \Delta H^0 - T\Delta S^0 \quad (7)$$

where  $K_d$  is the thermodynamic equilibrium constant ( $K_d = Q_d/C_e$ ),  $Q_d$  is the adsorption capacity at equilibrium (mg/g),  $C_e$  is the equilibrium concentration of the dye (mg/L),  $T$  is the absolute temperature (K),  $R$  is the gas constant (8.314 J/mol K),  $\Delta G^0$  is the change in Gibbs free energy (kJ/mol),  $\Delta H^0$  is the change in enthalpy (kJ/mol),  $\Delta S^0$  is the change in entropy (kJ/mol).

It can be seen from Table 2, the negative Gibbs free energy change ( $\Delta G^0$ ) and the positive value of  $\Delta H^0$ , indicate that the adsorption process is spontaneous and endothermic, and increase of temperature activates the adsorption sites. Further, the positive value of entropy change ( $\Delta S^0$ ), reflects randomness nature of process at the solid/solution interface and the molecules of acid violet 48 onto the sludge-straw adsorbent surface were organized in a more disorder state compared to those in the aqueous phase [14,38,39].

### 3.7. Adsorption kinetics

Adsorption kinetics is important for selecting optimum operating conditions. To evaluate the kinetic mechanism of the adsorption process, kinetic study of the adsorption of acid violet 48 from aqueous solution onto the sludge-straw was carried out by the well-known pseudo-first order, pseudo-second order and intra-particle models.

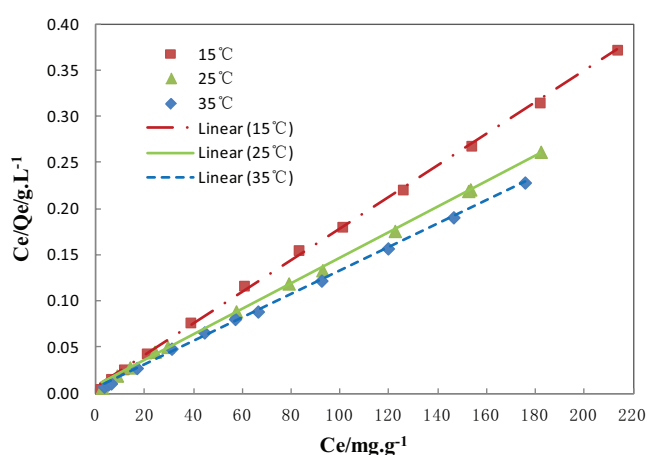


Fig. 8. Langmuir isotherm linear plot for the adsorption of acid violet 48.

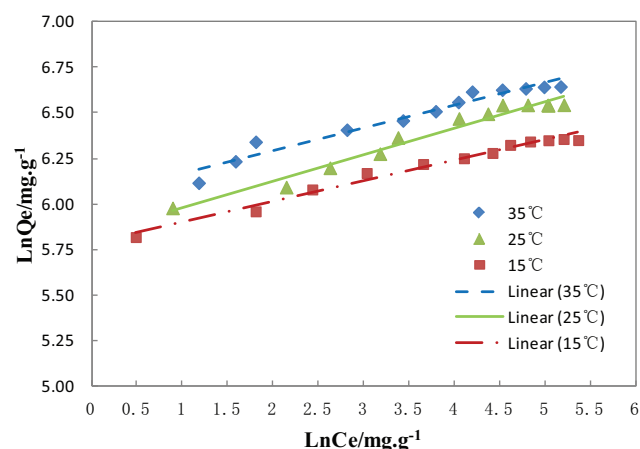


Fig. 9. Freundlich isotherm linear plot for the adsorption of acid violet 48.

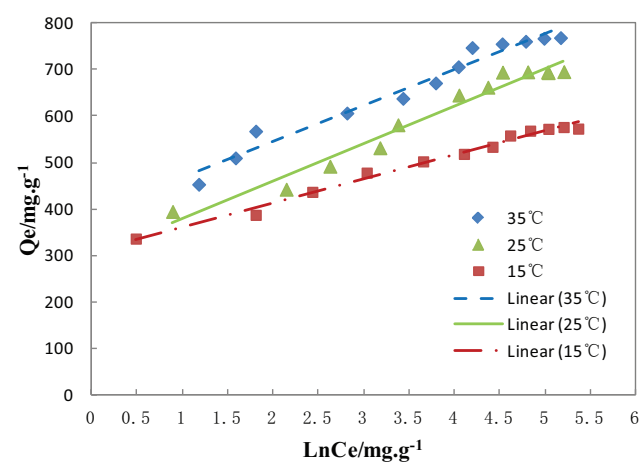


Fig. 10. Tempkin isotherm linear plot for the adsorption of acid violet 48.

Table 1  
Isotherm parameters for acid violet 48 adsorption at different temperatures

Temperature	Freundlich			Langmuir			Tempkin		
	$K$	$1/n$	$R^2$	$Q_m(\text{mg/g})$	$K_L(\text{L/mg})$	$R^2$	$A$	$B$	$R^2$
288 K	325.382	0.113	0.980	588.235	0.243	0.999	386.585	46.127	0.988
298 K	341.040	0.146	0.968	769.231	0.186	0.999	41.566	30.845	0.965
308 K	421.155	0.124	0.951	833.333	0.240	0.999	157.155	33.157	0.965

Table 2  
Thermodynamics parameters for acid violet 48 adsorption on sludge-straw adsorbent

$C_0$ (mg/L)	$\Delta H^0$ (kJ/mol)	$\Delta S^0$ (J/mol·K)	$\Delta G^0$ (kJ/mol)		
			288 K	298 K	308 K
320	53.42	203.61	-5.22	-7.25	-9.29
350	42.94	164.46	-4.43	-6.07	-7.72
380	37.02	142.51	-4.02	-5.44	-6.87
470	34.84	130.25	-2.67	-3.97	-5.27
500	31.75	118.22	-2.29	-3.47	-4.66

Pseudo-first order model is based on the assumption that the adsorption is controlled by diffusion step. The linear form of the pseudo-first order model is given as [40]:

$$\ln(q_e - q_t) = \ln q_e - k_1 t \quad (8)$$

where  $k_1$  is the pseudo-first order rate constant of the adsorption ( $\text{min}^{-1}$ ).

The linear form of pseudo-second order kinetic model given below was used by plotting  $t/q_t$  against  $t$ . The values of  $k_2$  and  $q_e$  can be determined experimentally from the slope and intercept of the plot of  $t/q_t$  vs.  $t$ , respectively. The pseudo-second order kinetic model is expressed as follows [41]:

$$\frac{t}{q_t} = \frac{1}{k_2 q_e^2} + \frac{t}{q_e} \quad (9)$$

where  $k_2$  is the equilibrium rate constant of pseudo second-order adsorption ( $\text{g/mg min}$ ) and  $q_e$  is the equilibrium adsorption capacity ( $\text{mg/g}$ ).

Intra-particle diffusion process is known as the rate-limiting step in many adsorption processes, which occurs in the pores of adsorbents, and the internal resistance to diffusive transport process is much higher than the external resistance. The intra-particle diffusion model is proposed by Weber and Morris to analyze the mechanism of the adsorption. This model is expressed as follows [8, 42]:

$$q_t = k_p t^{0.5} + C \quad (10)$$

where  $k_p$  is the adsorption rate constant of the intra-particle diffusion ( $\text{mg/g min}^{0.5}$ ).

Fitting the adsorption kinetics data of acid violet 48 with the above motioned three kinetics models [Eqs. (8)–(10)], the linear fitting curve and fitting equation are shown in

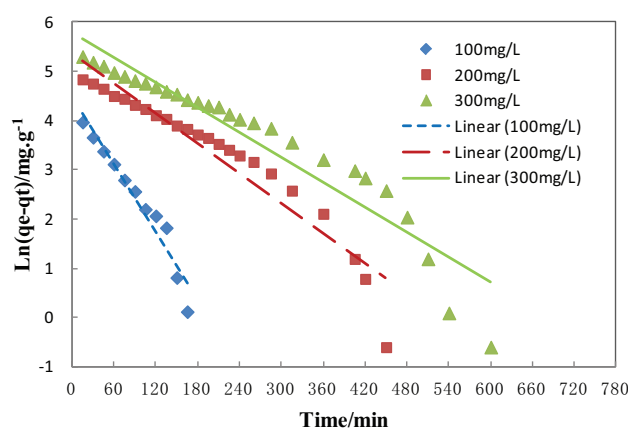


Fig. 11. Pseudo-first order model for the adsorption of acid violet 48 by sludge-straw adsorbent.

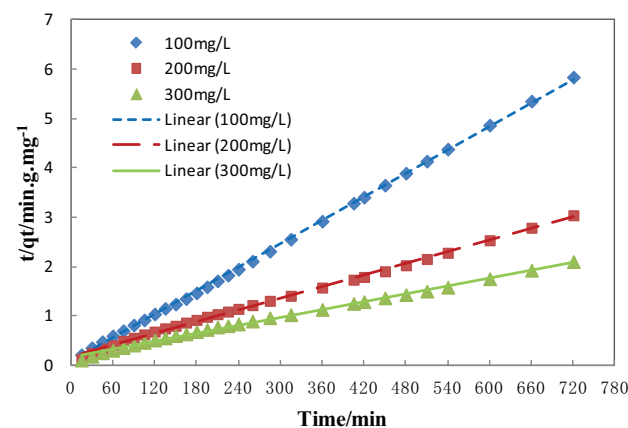


Fig. 12. Pseudo-second order model for the adsorption of acid violet 48 by sludge-straw adsorbent.

Figs. 11–13. The derived rate constants together with the corresponding linear regression correlation coefficient  $R^2$  values of three kinetic models can be obtained. The results are given in Table 3.

It was observed from the Table 3 and Figs. 11–13 that the best model to generate a good fit to the experimental data was the pseudo-second order model ( $R^2$ : 0.996, 0.998, 0.999, Table 3), followed by the pseudo-first order model ( $R^2$ : 0.902, 0.911, 0.943). The experimental  $q_e$  values (123.31, 236.84, 342.61 mg/g, Table 3) show a much better agreement with those obtained from the pseudo-second order model (125.79, 255.75, 374.53 mg/g, Table 3).

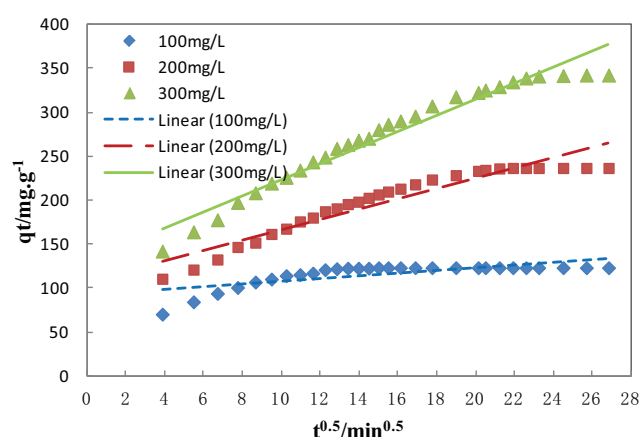


Fig. 13. Intra-particle diffusion kinetics of acid violet 48 onto sludge-straw adsorbents.

The intra-particle diffusion coefficient for the adsorption of acid violet 48 was calculated from the slope of the plot of square root of time ( $\text{min}^{0.5}$ ) vs. amount of dye adsorbed ( $\text{mg/g}$ ). Here, when the values of  $C$  equal to zero, namely, the plot passes through the origin, the intra-particle diffusion will be the sole rate limiting step. As seen from Fig.13, the plots do not pass through the origin. Therefore, it is not the sole rate-controlling step, besides the intra-particle diffusion, other processes such as surface adsorption and liquid film diffusion also involved in adsorption process.

### 3.8. Discussion

In the light of the isotherm and kinetics studies, it is observed that the adsorption thermodynamic and kinetic data were fitted well by Langmuir isotherm modern and second-order kinetics modern respectively. Therefore, we

Table 3  
Fitting kinetics parameters of acid violet 48

$C_0$ mg/L	$q^e$ mg/g	Pseudo first-order			Pseudo second-order			Intra-particle		
		$k_1$ 1/min	$q_e$ mg/g	$R^2$	$k_2$ g/mg min	$q_e$ mg/g	$R^2$	$k_p$ mg/g min <sup>0.5</sup>	$C$	$R^2$
100	123.31	0.02302	88.23	0.943	8.778E-04	125.79	0.999	1.570	92.08	0.557
200	236.84	0.01016	213.79	0.911	8.264E-05	255.75	0.998	5.816	108.3	0.906
300	342.61	0.00847	329.31	0.902	4.243E-05	374.53	0.996	9.095	132.6	0.953

Note:  $q^e$  and  $q_e$  represent the equilibrium adsorption capacity obtained by experiment and calculation respectively.

Table 4  
Comparison of the maximum adsorption capacities of dyes onto various adsorbents

Adsorbent	Dye	$q_m$	Ref.
Sludge-straw activated carbon	Acid violet 48	833.33 mg/g	This work
3D rGO macrostructure	Acid red 1	277.01 mg/g	[2]
3D rGO macrostructure	Methylene blue	302.11 mg/g	[2]
Pyrolyzed petrified sediment	Trypan blue	345 mg/g	[8]
Activated Mangifera indica Saw Dust	Congo red	45.5 mg/g	[12]
Camellia seed powder	Methylene blue	9.19 mg/g	[13]
Camellia seed powder	Methyl violet	3.08 mg/g	[13]
Platanus orientalis leaf powder	Methylene blue	114.94 mg/g	[14]
Safi decanted clay	Acid orange 52	88.70 mg/g	[15]
Safi decanted clay	Malachite green	169.68 mg/g	[15]
Surfactant modified bentonite clay	Methylene blue	399.74 $\mu\text{mol/g}$	[16]
Surfactant modified bentonite clay	Crystal violet	365.11 $\mu\text{mol/g}$	[16]
Surfactant modified bentonite clay	Rhodamine B	324.36 $\mu\text{mol/g}$	[16]
Eichhornia charcoal	Crystal violet	58.13 mg/g	[18]
Modified Eichhornia crassipes	Crystal violet	116.3 mg/g	[19]
Eichhornia charcoal	Congo red	103.2 mg/g	[20]
Sludge-straw activated carbon	Acid turquoise blue 2G	1.5738 mmol/g	[32]
Sludge-straw activated carbon	Acid scarlet 3R	111.11 mg/g	[33]
MCM-41	Safranin	68.8 mg/g	Reference 43

can consider that the surface of sludge-straw adsorbent is homogeneous and contains structurally and energetically active sites. Each site can hold at most one molecule of dye (mono-layer coverage only), and there are no interactions between adsorbate molecules on adjacent sites. The adsorption is an endothermic and spontaneous process. The adsorption rate of acid violet 48 is determined by the square value of the number of hollow sites on the surface of the adsorbent. The adsorption process is controlled by the mechanism of chemical adsorption, which involves the electron sharing or electron transfer between the adsorbent and the adsorbate, so the adsorption of acid violet 48 by the sludge-straw adsorbent is complex, and includes more than one mechanism, such as external liquid film diffusion, surface adsorption, and intra-particle diffusion.

### 3.9. Comparison of various adsorbents and dyes

The maximum monolayer adsorption capacities of the sludge-straw adsorbent in this work were compared to the previous work (Table 4). From the comparison it can be concluded that the adsorbent derived from sludge and straw is effective for the removal of dyes from aqueous solution.

### 3.10. Regeneration of sludge-straw adsorbent adsorbed and saturated

In order to know the regeneration ratio of sludge-straw adsorbent, the regeneration experiment was carried out. Firstly, the saturated adsorbent was taken, 200 ml of 10% sodium hydroxide solution was added and stirred at 200 rpm for 30 min, and then filtered to remove alkali solution, it was repeated once in accordance with the above operation. Secondly, the adsorbent was filtered and cleaned using 90–100°C water until pH value was close to 7. Finally, the adsorbent was dried at 105°C in the oven, and the regeneration rate was determined. The regeneration rate of saturated adsorbent was about 43%.

## 4. Conclusions

In this study, excess sludge and corn straw can be changed into a prospective adsorbent for the removal of the dyestuffs from its aqueous solutions. The adsorbent showed a high performance for the adsorption of acid violet 48, and the maximum amount of acid violet 48 adsorbed ( $Q_m$ ) achieved 833.333 mg/g at 308 K. The adsorption of acid violet 48 onto sludge-straw adsorbent was found to be consistent with the assumption of Langmuir monolayer. Thermodynamic parameter showed that the process is endothermic and spontaneous. The adsorption of acid violet 48 was best described by pseudo-second order kinetic model.

## Acknowledgements

This work was financially supported by Shanxi Science and Technology Agency Research Project (No. 2015011018) and sponsored by the Fund for Shanxi Key Subjects Construction.

## References

- [1] P. Tian, X.Y. Han, G.L. Ning, H.X. Fang, J.W. Ye, W.T. Gong, Y. Lin, Synthesis of porous hierarchical MgO and its superb adsorption properties, *ACS Appl. Mater. Inter.*, 5 (2013) 12411–12418.
- [2] K. Han, S.O. Kang, S. Park, H.S. Park, Adsorption isotherms and kinetics of cationic and anionic dyes on three-dimensional reduced graphene oxide macrostructure, *J. Ind. Eng. Chem.*, 21 (2015) 1191–1196.
- [3] L. Lu, J. Li, J. Yu, P. Song, Dickon H.L. Ng., A hierarchically porous  $MgFe_2O_4/c-Fe_2O_3$  magnetic microspheres for efficient removals of dye and pharmaceutical from water, *Chem. Eng. J.*, 283 (2016) 524–534.
- [4] Ö. Demirbaş, M. Alkan, Adsorption kinetics of a cationic dye from wastewater, *Desal. Water Treat.*, 53 (2015) 3623–3631.
- [5] W.S. Wan Ngah, L.C. Teong, M.A.K.M. Hanafiah, Adsorption of dyes and heavy metal ions by chitosan composites: a review, *Carbohydr. Polym.*, 83 (2011) 1446–1456.
- [6] H. Karaer, I. Uzun, Adsorption of basic dyestuffs from aqueous solution by modified chitosan, *Desal. Water Treat.*, 51 (2013) 2294–2305.
- [7] F.C. Tsai, N. Ma, T.C. Chiang, L.C. Tsai, J.J. Shi, Y. Xia, T. Jiang, S.K. Su, F.S. Chuang, Adsorptive removal of methyl orange from aqueous solution with crosslinking chitosan microspheres, *J. Water Process Eng.*, 1 (2014) 2–7.
- [8] T. Sismanoglu, A.Z. Aroguz, Adsorption kinetics of diazo-dye from aqueous solutions by using natural origin low-cost biosorbents, *Desal. Water Treat.*, 54 (2015) 736–743.
- [9] M.T. Sulaka, C.H. Yatmaz, Removal of textile dyes from aqueous solutions with eco-friendly biosorbent, *Desal. Water Treat.*, 37 (2012) 169–177.
- [10] M.C. Shih, Kinetics of the batch adsorption of methylene blue from aqueous solutions onto rice rusk: Effect of acid-modified process and dye concentration, *Desal. Water Treat.*, 154 (2012) 337–346.
- [11] F.K. Bangash, S. Alam, Adsorption of acid blue 1 on activated carbon produced from the wood of *Ailanthus altissima*, *Braz. J. Chem. Eng.*, 26 (2009) 275–285.
- [12] P.R. Patil, Y.V. Marathe, V.S. Shrivastava, Evaluation of the adsorption kinetics and equilibrium for the potential removal of Congo red dye from aqueous medium by using a biosorbent, *Brit. J. Appl. Sci. Technol.*, 6 (2015) 557–573.
- [13] C.C. Wang, J. Zhang, P. Wang, H. Wang, H. Yan, Adsorption of methylene blue and methyl violet by camellia seed powder: kinetic and thermodynamic studies, *Desal. Water Treat.*, 53 (2015) 3681–3690.
- [14] M. Peydayesh, A. Rahbar-Kelishami, Adsorption of methylene blue onto *Platanus orientalis* leaf powder: kinetic, equilibrium and thermodynamic studies, *J. Ind. Eng. Chem.*, 21 (2015) 1014–1019.
- [15] R. Elmoubarki, F.Z. Mahjoubi, H. Tounsadi, J. Moustadraf, M. Abdennouri, A. Zouhri, A. El Albani, N. Barka, Adsorption of textile dyes on raw and decanted Moroccan clays: kinetics, equilibrium and thermodynamics, *Water Resour. Ind.*, 9 (2015) 16–29.
- [16] T.S. Anirudhan, M. Ramachandran, Adsorptive removal of basic dyes from aqueous solutions by surfactant modified bentonite clay (organoclay): kinetic and competitive adsorption isotherm, *Process Saf. Environ.*, 95 (2015) 215–225.
- [17] N. Barka, A. Assabane, A. Nounah, L. Laanab, Y. AïtIchou, Removal textile dyes from aqueous solution by natural phosphate as new adsorbent, *Desalination*, 235 (2009) 264–275.
- [18] S. Kaur, S. Rani, R.K. Mahajan, Adsorptive removal of dye crystal violet onto low-cost carbon produced from *Eichhornia* plant: kinetic, equilibrium, and thermodynamic studies, *Desal. Water Treat.*, 53 (2015) 543–556.
- [19] S. Kaur, S. Rani, R.K. Mahajan, Adsorption of dye crystal violet onto surface-modified *Eichhornia crassipes*, *Desal. Water Treat.*, 53 (2015) 1957–1969.
- [20] S. Kaur, S. Rani, R.K. Mahajan, V.K. Gupta, Modification of surface behaviour of *Eichhornia crassipes* using surface active agent: An adsorption study, *J. Ind. Eng. Chem.*, 21 (2015) 189–197.

- [21] K.G. Bhattacharyya, S.S. Gupta, G.K. Sarma, Kinetics, equilibrium isotherms and thermodynamics of adsorption of Congo red onto natural and acid-treated kaolinite and montmorillonite, *Desal. Water Treat.*, 53 (2015) 530–542.
- [22] A. Ebrahimi, E. Pajootan, M. Arami, H. Bahrami, Optimization, kinetics, equilibrium, and thermodynamic investigation of cationic dye adsorption on the fish bone, *Desal. Water Treat.*, 53 (2015) 2249–2259.
- [23] Ö. Demirbaş, Y. Turhana, M. Alkan, Thermodynamics and kinetics of adsorption of a cationic dye onto sepiolite, *Desal. Water Treat.*, 54 (2015) 707–714.
- [24] J. Mittal, V. Thakur, A. Mittal, Batch removal of hazardous azo dye Bismark Brown R using waste material hen feather, *Ecol. Eng.*, 60 (2013) 249–253.
- [25] A. Mittal, V. Thakur, V. Gajbe, Adsorptive removal of toxic azo dye Amido Black 10B by hen feather, *Environ. Sci. Pollut. Res.*, 20 (2013) 260–269.
- [26] A. Mittal, V. Thakur, J. Mittal, H. Vardhan, Process development for the removal of hazardous anionic azo dye Congo Red from wastewater by using hen feather as potential adsorbent, *Desal. Water Treat.*, 52 (2014) 227–237.
- [27] A. Mittal, J. Mittal, L. Kurup, Utilization of Hen Feathers for the adsorption of Indigo Carmine from simulated effluent, *J. Environ. Prot. Sci.*, 1 (2007) 92–100.
- [28] S. Sadaf, H.N. Bhatti, Batch and fixed bed column studies for the removal of Indosol Yellow BG dye by peanut husk, *J. Taiwan Inst. Chem. Eng.*, 45 (2014) 541–553.
- [29] S. Sadaf, H.N. Bhatti, Evaluation of peanut husk as a novel, low cost biosorbent for the removal of Indosol Orange RSN dye from aqueous solutions: Batch and fixed bed studies, *Clean Technol. Environ. Policy*, 16 (2014) 527–544.
- [30] K. Huang, B.X. Du, The research on preparation methods of sludge-based adsorbent and its application in water treatment, *Adv. Mater. Res.*, 798–799 (2013) 1166–1169.
- [31] F. Li, T. Lei, Y.P. Zhang, J.Z. Wei, Y. Yang, Preparation, characterization of sludge adsorbent and investigations on its removal of hydrogen sulfide under room temperature, *Front. Environ. Sci. Eng.*, 9 (2015) 190–196.
- [32] X.L. Ren, X.H. Lai, K.J. Zhu, Y. Sun, D.L. He, Removal of acid turquoise blue 2G from aqueous solution by adsorbent derived from sludge and straw: kinetic, isotherm and thermodynamic study, *Desal. Water Treat.*, 57 (2016) 440–448.
- [33] X.L. Ren, L. Yang, M. Liu, Kinetic and thermodynamic studies of acid scarlet 3R adsorption onto low-cost adsorbent developed from sludge and straw, *Chin. J. Chem. Eng.*, 22 (2014) 208–213.
- [34] I. Langmuir, The adsorption of gases on plane surfaces of glass, mica, and platinum, *J. Am. Chem. Soc.*, 40 (1918) 1361–1403.
- [35] H. Freundlich, Über die Adsorption in Lösungen, *Zeitschrift für physikalische Chemie [About the adsorption in solution]*, 57 (1906) 385–470.
- [36] L. Chen, B. Bai, Equilibrium, kinetic, thermodynamic, and in situ regeneration studies about methylene blue adsorption by the raspberry-like TiO<sub>2</sub>@yeast microspheres, *Ind. Eng. Chem. Res.*, 52 (2013) 15568–15577.
- [37] I.E. Saliby, L. Erdei, J.H. Kim, H.K. Shon, Adsorption and photocatalytic degradation of methylene blue over hydrogen-titanate nanofibres produced by a peroxide method, *Water Res.*, 47 (2013) 4115–4125.
- [38] D. Pathania, S. Sharma, P. Singh, Removal of methylene blue by adsorption onto activated carbon developed from *Ficus carica* bast, *Arabian J. Chem.*, 10 (2017) s1445–s1451.
- [39] J. Zhang, D. Cai, G. Zhang, C. Cai, C. Zhang, G. Qiu, K. Zheng, Z. Wu, Adsorption of methylene blue from aqueous solution onto multiporous palygorskite modified by ion beam bombardment: effect of contact time, temperature, pH and ionic strength, *Appl. Clay Sci.*, 83–84 (2013) 137–143.
- [40] S. Lagergren, Zur theorie der sogenannten adsorption gelöster stoffe, *Kungliga Svenska Vetenskapsakademiens [About the theory of so-called adsorption of soluble substances]*, *Handlingar Band*, 24 (1898) 1–39.
- [41] S.K. Theydan, M.J. Ahmed, Adsorption of methylene blue onto biomass-based activated carbon by FeCl<sub>3</sub> activation: Equilibrium, kinetics, and thermodynamic studies, *J. Anal. Appl. Pyrol.*, 97 (2012) 116–122.
- [42] W.J. Weber, J.C. Morris, Kinetics of adsorption on carbon from solution, *J. Sanit. Eng. Div. Am. Soc. Civil Eng.*, 89 (1963) 31–60.
- [43] S. Kaur, S. Rani, R.K. Mahajan, M. Asif, V.K. Gupta, Synthesis and adsorption properties of mesoporous material for the removal of dye safranin: Kinetics, equilibrium, and thermodynamics, *J. Ind. Eng. Chem.*, 22 (2015) 19–27.